iScience

CellPress
OPEN ACCESS

Article

CircMEF2C(2, 3) modulates proliferation and adipogenesis of porcine intramuscular preadipocytes by miR-383/671-3p/*MEF2C* axis

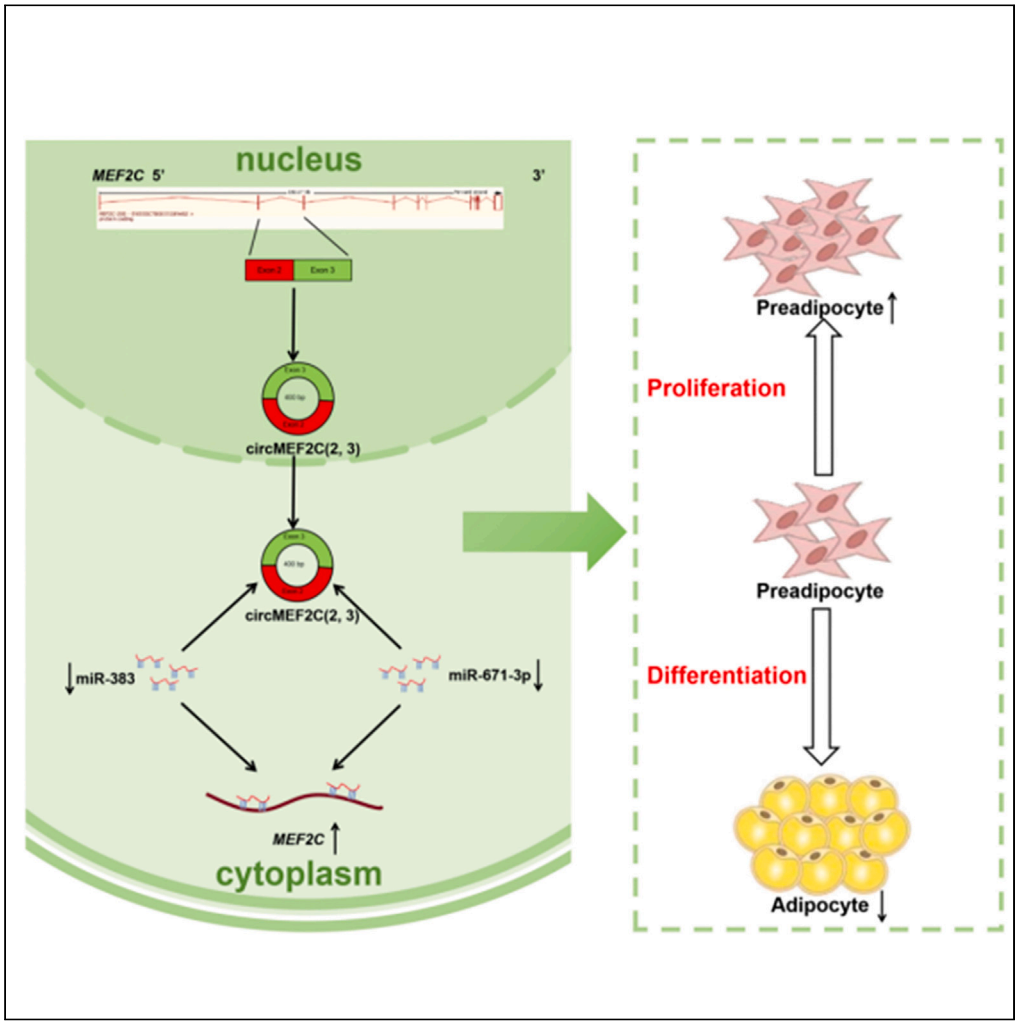

Xiaoyin Rong, Ruixiao Li, Tianye Gong, ..., Bugao Li, Yang Yang, Xiaohong Guo

yangyangyh@sxau.edu.cn (Y.Y.)
g_xiaohong@126.com (X.G.)

Highlights

CircMEF2C is formed through the reverse splicing of the 2 to 3 exons of *MEF2C* gene

CircMEF2C acts as a key regulator of proliferation and adipogenic differentiation

CircMEF2C sponges miR-383 and miR-671-3p to maintain *MEF2C* expression

Rong et al., iScience 27, 109710
May 17, 2024 © 2024 The Authors. Published by Elsevier Inc.
https://doi.org/10.1016/j.isci.2024.109710

iScience

CellPress
OPEN ACCESS

Article

CircMEF2C(2, 3) modulates proliferation and adipogenesis of porcine intramuscular preadipocytes by miR-383/671-3p/*MEF2C* axis

Xiaoyin Rong,[1,2,3] Ruixiao Li,[1,2,3] Tianye Gong,[1,2] Haonan Li,[1,2] Xiaolei Zhao,[1,2] Guoqing Cao,[1,2] Meng Li,[1,2] Bugao Li,[1,2] Yang Yang,[1,2,*] and Xiaohong Guo[1,2,4,*]

SUMMARY

Circular RNA is a special category of non-coding RNA that has emerged as epigenetic regulator of adipose tissue development. However, the mechanism governing intramuscular adipogenesis of circRNA remains largely uncharted. In this study, circMEF2C(2, 3), looped by *MEF2C* exons 2 and 3, was identified from the pig *MEF2C* gene. Expression of circMEF2C(2, 3) is upregulated in early stage of intramuscular adipogenesis and muscular tissue of lean pigs (DLY pig). Subsequently, overexpression or knockdown of circMEF2C(2, 3) reflected that it participates in promoting proliferation and inhibiting adipogenic differentiation in porcine intramuscular preadipocytes and murine C3H10T1/2 cells. Mechanically, circMEF2C(2, 3) competitively combined with miR-383 and miR-671-3p to the 3′-UTR of *MEF2C*, which maintains *MEF2C* expression in regulating proliferation and adipogenesis. In summary, circMEF2C(2, 3) is a key regulator in the proliferation and adipogenic differentiation of intramuscular adipogenesis, suggesting its potential as a multi-target strategy for adipose development and associated diseases.

INTRODUCTION

Adipose tissue plays a critical role as the body's primary energy store, offering organ protection and hormonal regulation. Nevertheless, excessive adipose accumulation contributes to obesity cardiovascular diseases, and diabetes risks.[1,2] Therefore, further research is necessary for a comprehensive understanding regulation of adipocyte differentiation. Pigs, given their physiological and metabolic similarities to humans, particularly in adipose generation and metabolism, serve as valuable models for studying these mechanisms. Additionally, the thickness of subcutaneous fat and intramuscular fat (IMF) content profoundly affects pork quality.[3,4] IMF influences marbling scores and contributes to meat flavor through its adipose composition.[5,6] Therefore, exploring adipocyte generation in IMF holds immense significance for both livestock production and human health.

Adipocyte generation is a complex process involving pluripotent stem cell differentiation into mature adipocytes, orchestrated by various regulation factors. Ultimately, these factors regulate gene networks and signaling pathways.[7] Epigenetic regulators, including non-coding RNAs (ncRNAs), especially circular RNAs (circRNAs), have gained prominence due to their enhanced stability and widespread presence in various tissues and species.[8,9] CircRNAs have been shown to modulate gene expression through miRNA interactions,[10,11] protein binding,[12,13] and protein translation,[14,15] impacting various biological processes like cancer, obesity, and immunity. Li et al. have utilized RNA sequencing to analyze pig muscle tissue with varying IMF content, leading to the identification of differential circRNAs and demonstrated circPPARA regulates porcine intramuscular adipogenesis via miR-429.[16] While numerous circRNAs associated with IMF formation have been predicted and identified, their specific roles and mechanisms in adipose formation still require further investigation.

MEF2C, a MADS-box transcription factor, plays an integral role in cell development through binding to MEF2 sites rich in A/T sequences to activate or enhance gene expression.[17–19] Previous research has identified *MEF2C* as a crucial transcription factor for various cell types, including muscle cells, nerve cells, chondrocytes, immune cells, and endothelial cells. Our findings also indicate that *MEF2C* operates as a downstream target gene of *HMG20A* and experiences co-regulation by *HMG20A* and *LSD1*, implicating its involvement in adipose generation.[20] Nonetheless, the upstream regulatory mechanisms governing *MEF2C* remain unexplored. RNA sequencing was performed the expression of circMEF2C(2, 3) decreased in obese-type pig breeds (Mashen) compared with lean-type pig breeds (Large White).[21] Hence, the specific regulatory role of circMEF2C(2, 3) in muscle needs to be further revealed.

[1]College of Animal Science, Shanxi Agricultural University, Jinzhong 030801, P.R. China
[2]Key Laboratory of Farm Animal Genetic Resources Exploration and Breeding of Shanxi Province, Jinzhong 030801, P.R. China
[3]These authors contributed equally
[4]Lead contact
*Correspondence: yangyangyh@sxau.edu.cn (Y.Y.), g_xiaohong@126.com (X.G.)
https://doi.org/10.1016/j.isci.2024.109710

This is an open access article under the CC BY-NC license (http://creativecommons.org/licenses/by-nc/4.0/).

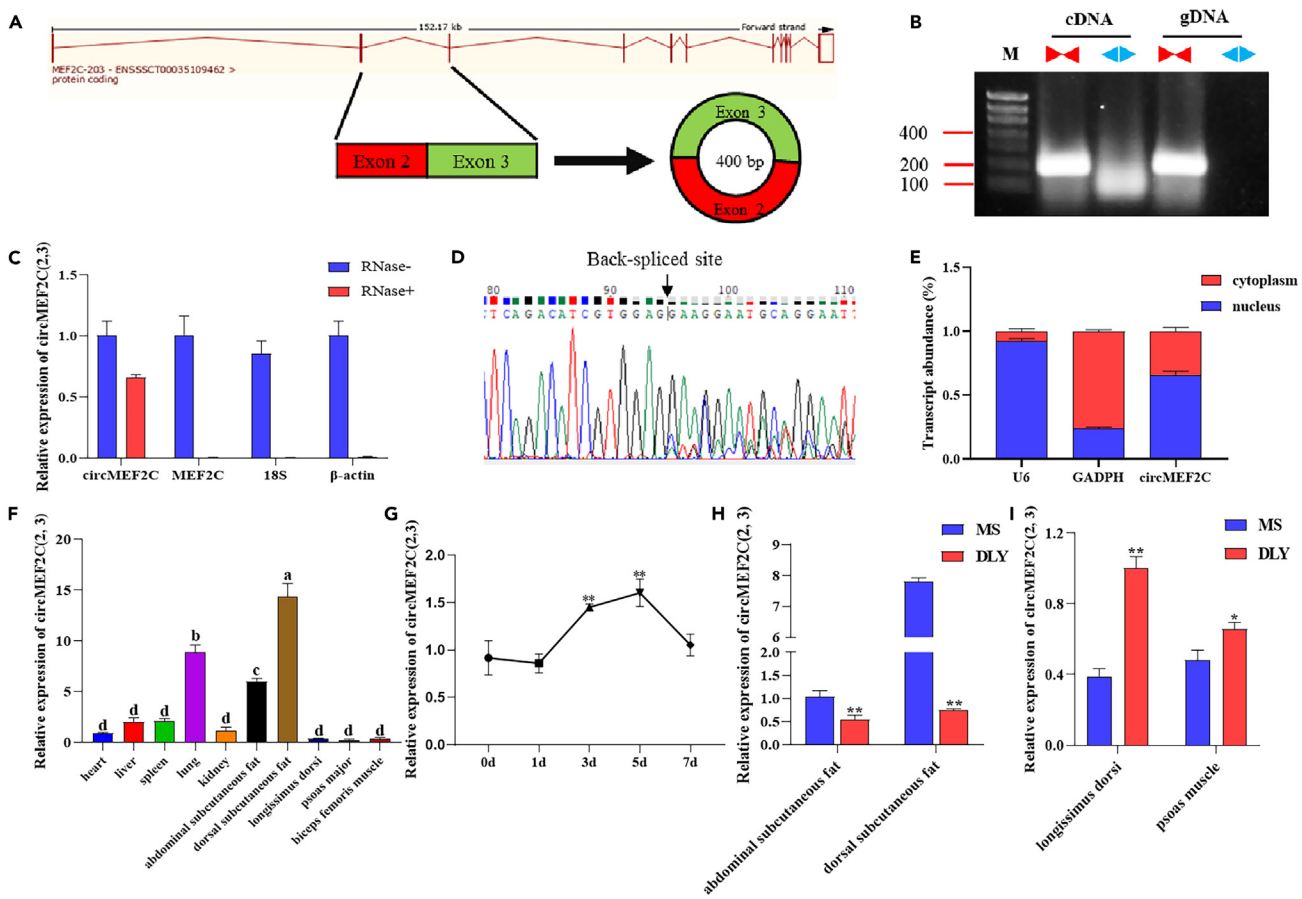

Figure 1. Identification and expression analysis of circMEF2C(2, 3)

(A) Diagram illustrating the generation of circMEF2C(2, 3) from the *MEF2C* gene.

(B) Detection of circMEF2C(2, 3) in cDNA and gDNA using divergent and convergent primers via PCR.

(C) Detection of circMEF2C(2, 3) and *MEF2C* expression after RNase R digestion (37°C, 50 min).

(D) Confirmation of the back-splice junction (BSJ) of circMEF2C(2, 3) through Sanger sequencing.

(E) Subcellular localization analysis of circMEF2C(2, 3).

(F) Tissue expression profile of circMEF2C(2, 3).

(G) Expression patterns of circMEF2C(2, 3) during adipogenesis.

(H) Expression of circMEF2C(2, 3) in adipose tissue of MS pigs and DLY pigs.

(I) Expression of circMEF2C(2, 3) in muscle tissue of MS pigs and DLY pigs.

In our research, porcine intramuscular preadipocytes were isolated and cultivated to investigate the regulatory role of circMEF2C(2, 3) in adipogenesis. We further analyzed its mechanism of action and found that it functions as a miR-383 and miR-671-3p sponge, operating through the competitive endogenous RNA (ceRNA) mechanism, thereby attenuating *MEF2C* regulation. This study demonstrates that circMEF2C(2, 3) inhibits adipogenesis, contributing unique insights into the function of circRNAs in lipid metabolism.

RESULTS

Identification and expression analysis of CircMEF2C(2, 3)

CircMEF2C(2, 3) is looped by *MEF2C* exons 2 and 3, measuring 400 nt in length. Verified by Sanger sequencing, the black arrow indicates the splice site of circMEF2C(2, 3) in the head and tail (Figures 1A and 1D). Subsequent polymerase chain reaction (PCR) showed that circMEF2C(2, 3) could be amplified using divergent primers in cDNA reverse-transcribed from random hexamers but not with gDNA primers (Figure 1B). We employed Ribonuclease R (RNase R) to assess the stability of circMEF2C(2, 3). Following RNase R treatment, almost no linear mRNA was detected, yet the expression level of circMEF2C(2, 3) remained around 60%, indicating its higher stability compared to linear mRNA (Figure 1C). From cytoplasmic and nucleus separation experiments, it was discovered that circMEF2C(2, 3) is expressed in both the cytoplasm and nucleus (Figure 1E). We further explored the relative expression of circMEF2C(2, 3) in various pig tissues using quantitative real-time polymerase chain reaction (real-time qPCR, RT-qPCR), revealing its highest expression in dorsal subcutaneous fat, followed by lung and abdominal fat (Figure 1F). Furthermore, during the induction of adipogenic differentiation in porcine intramuscular preadipocytes,

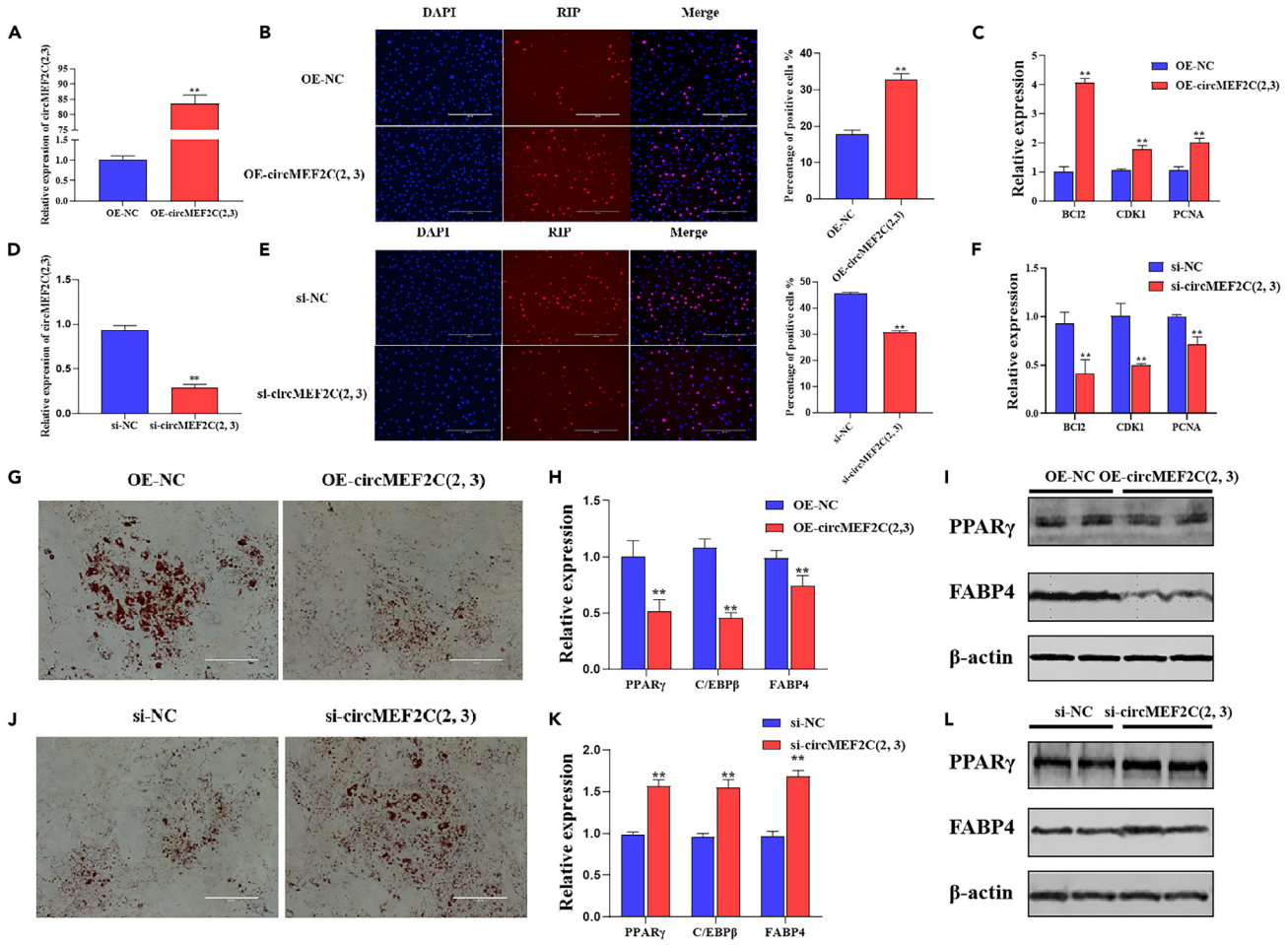

Figure 2. CircMEF2C(2, 3) enhances proliferation and suppresses adipogenic differentiation in porcine intramuscular preadipocytes

(A) Detection of circMEF2C(2, 3) overexpression efficiency in porcine intramuscular preadipocytes.

(B) Differences in EdU staining following circMEF2C(2, 3) overexpression.

(C) Alterations in mRNA expression of proliferation-related genes following circMEF2C(2, 3) overexpression.

(D) Evaluation of si-circMEF2C(2, 3) interference efficiency in porcine intramuscular preadipocytes.

(E) Differences in EdU staining following circMEF2C(2, 3) interference.

(F) Alterations in mRNA expression of proliferation-related genes following circMEF2C(2, 3) interference.

(G) Representative results of oil red O staining following circMEF2C(2, 3) overexpression.

(H) Alterations in mRNA expression of adipogenic factors following circMEF2C(2, 3) overexpression.

(I) Alterations in protein expression of adipogenic factors following circMEF2C(2, 3) overexpression.

(J) Representative results of oil red O staining following circMEF2C(2, 3) interference.

(K) Alterations in mRNA expression of adipogenic factors following circMEF2C(2, 3) interference.

(L) Alterations in protein expression of adipogenic factors following circMEF2C(2, 3) interference.

circMEF2C(2, 3) displayed a trend of increasing expression, with peak levels observed at 5 days of adipogenesis (Figure 1G). Additionally, circMEF2C(2, 3) was detected in different breeds of pigs and it was found that it is expressed more in the muscle of lean pigs (DLY) (Figures 1H and 1I). These combined results strongly indicate circMEF2C(2, 3)'s involvement in adipogenic differentiation of IMF.

CircMEF2C(2, 3) enhances proliferation and suppresses adipogenic differentiation in porcine intramuscular preadipocytes

To explore the influence of circMEF2C(2, 3) on cell proliferation and adipogenic differentiation in porcine intramuscular preadipocytes, we first constructed an overexpression vector for circMEF2C(2, 3) and assessed its overexpression efficiency (Figure 2A). Notably, EdU staining revealed a substantial increase in the proportion of positive cells (Figure 2B), and RT-qPCR indicated a significant upregulation in the expression of proliferation-related genes, namely *BCl2*, *CDK1*, and *PCNA*, due to circMEF2C(2, 3) overexpression (Figure 2C). Conversely, the introduction of siRNA into the cells yielded contrasting results (Figures 2D–2F). Subsequently, following the induction of adipogenic differentiation in cells with overexpressed circMEF2C(2, 3), oil red O staining exhibited a significant reduction in lipid droplets within the overexpression

group (Figure 2G). Moreover, the expression of adipogenic marker genes such as *PPARγ*, *C/EBPβ*, and *FABP4* was significantly decreased (Figure 2H), and the outcomes of Western blot findings indicated that PPARγ and FABP4 expression levels were considerably decreased compared with the control group (Figure 2I). Meanwhile, the interference of circMEF2C(2, 3) yielded results contrary to those observed in the overexpression group (Figures 2J–2L). These findings collectively affirm that circMEF2C(2, 3) promotes cell proliferation while inhibiting adipogenic differentiation in porcine intramuscular preadipocytes.

CircMEF2C(2, 3) regulates proliferation and adipogenesis in murine C3H10T1/2 cells

Since circMEF2C(2, 3) is conserved among different species, we conducted homology analysis, and the results showed a 94.2% homology between porcine circMEF2C(2, 3) and murine circMEF2C(2, 3), and a 97.2% homology between porcine circMEF2C(2, 3) and human circMEF2C(2, 3) (Figure 3A), Therefore, we examined the effect of circMEF2C(2, 3) on the proliferation and adipogenesis in Murine C3H10T1/2 mesenchymal stem cells. We first examined the overexpression efficiency of circMEF2C(2, 3) (Figure 3B). EdU staining revealed a significant increase in cell proliferation in C3H10T1/2 cells (Figure 3C), while RT-qPCR unveiled a significant upregulation of the expression of *BCl2*, *CDK1*, and *PCNA* (Figure 3D). Oil red O staining indicated a significant reduction in lipid droplets within the overexpression group (Figure 3H). Furthermore, the expression of PPARγ, C/EBPβ, and FABP4 showed significant decreases (Figures 3I and 3J). The interference of circMEF2C(2, 3) yielded results contrasting with those of the overexpression group (Figures 3E–3G and 3K–3M). These collective findings confirm that circMEF2C(2, 3) promotes cell proliferation and inhibits adipogenic differentiation in murine C3H10T1/2 cells.

CircMEF2C(2, 3) acts as a miR-383 and miR-671-3p sponge

To investigate the downstream mechanism of circMEF2C(2, 3), we utilized miRanda and RNAhybrid to search for the miRNAs with which it may interact (Figure 4A). Subsequent studies demonstrated that overexpression of circMEF2C(2, 3) led to significantly reduced expression of miR-383 and miR-671-3p, whereas interference with circMEF2C(2, 3) resulted in the opposite effect (Figures 4B and 4C). By employing the RNAhybrid software to predict the binding sites of circMEF2C(2, 3) with miR-383 and miR-671-3p, we constructed plasmids containing both wild-type and mutant-type circMEF2C(2, 3) sequences (Figures 4D and 4H). Dual luciferase reporter gene assays provided evidence that, in comparison to other groups, the luciferase activity of the psiCHECK2-circMEF2C(2, 3)-WT + miR-383 mimics group and psiCHECK2-circMEF2C(2, 3)-WT + miR-671-3p mimics group significantly decreased (Figures 4E and 4I), indicating the binding of circMEF2C(2, 3) to miR-383 and miR-671-3p. Further expression pattern analysis revealed an initial increase and subsequent decrease in miR-383 and miR-671-3p levels during the adipogenic differentiation induction of porcine intramuscular preadipocytes (Figures 4F and 4J). Furthermore, miR-383 and miR-671-3p were significantly lower in MS pigs compared to DLY pigs (Figures 4G and 4K), contrasting the expression pattern of circMEF2C(2, 3) (Figures 1G and 1H).

miR-383 and miR-671-3p suppress proliferation and promote adipogenic differentiation

Subsequently, we investigated the function of miR-383 and miR-671-3p. EdU staining and RT-qPCR showed that overexpression of miR-383 and miR-671-3p promoted cell proliferation (Figures 5A and 5B). Furthermore, oil red O staining and RT-qPCR demonstrated that miR-383 and miR-671-3p inhibited adipogenic differentiation (Figures 5D and 5E). Transfecting miR-383 or miR-671-3p inhibitors effectively reversed these effects (Figures 5A, 5C, 5D, and 5F).

CircMEF2C (2,3) affects cell proliferation and adipogenesis through miR-383 and miR-671-3p

To investigate the impact of circMEF2C(2, 3) and the interplay with miR-383/miR-671-3p on cell proliferation and adipogenic differentiation, rescue experiments were designed. EdU staining and RT-qPCR demonstrated that the addition of the miR-383 inhibitor or miR-671-3p inhibitor effectively rescued the inhibitory effect of si-circMEF2C(2,3) on cell proliferation (Figures 6A and 6B). Oil red O staining and RT-qPCR demonstrated that the miR-383 inhibitor or miR-671-3p inhibitor effectively counteracted the promotional impact of si-circMEF2C(2, 3) on adipogenic differentiation (Figures 5C and 5D). Collectively, these findings imply that circMEF2C(2, 3) facilitates proliferation and inhibits adipogenic differentiation by interacting with miR-383 and miR-671-3p.

miR-383 and miR-671-3p bind to the 3′-UTR of *MEF2C*

In this study, RNA22, miRWalk, miRNAMAap, and miRDB databases were employed for predicting the downstream target genes of miR-383 and miR-671-3p. By intersection analysis and Venn diagram, we established the circMEF2C(2, 3) ceRNA regulatory network. This analysis revealed that the *MEF2C* gene is a common target of both miR-383 and miR-671-3p, and notably, it is also the source gene of circMEF2C(2, 3) (Figures 7A–7C and 1A). Our experiments demonstrated that the overexpression of miR-383 or miR-671-3p in cells resulted in a significant reduction in *MEF2C* expression (Figure 7D). Conversely, the interference with miR-383 or miR-671-3p in cells led to a significant increase in *MEF2C* expression (Figure 7E). Additionally, we observed that the overexpression of circMEF2C(2, 3) in cells significantly enhanced the expression of *MEF2C* (Figure 7F). In contrast, interfering with circMEF2C(2, 3) in cells significantly reduced *MEF2C* expression (Figure 7G). Using the RNAhybrid software, we predicted that the seed sequences of miR-383 and miR-671-3p could form secondary structures with the 3′UTR of *MEF2C* through base complementarity. To validate this, we constructed both wild-type and mutant-type plasmids of *MEF2C* (Figures 7H and 7J). Subsequent dual-luciferase reporter gene analysis revealed the binding of *MEF2C* with miR-383 and miR-671-3p (Figures 7I and 7K).

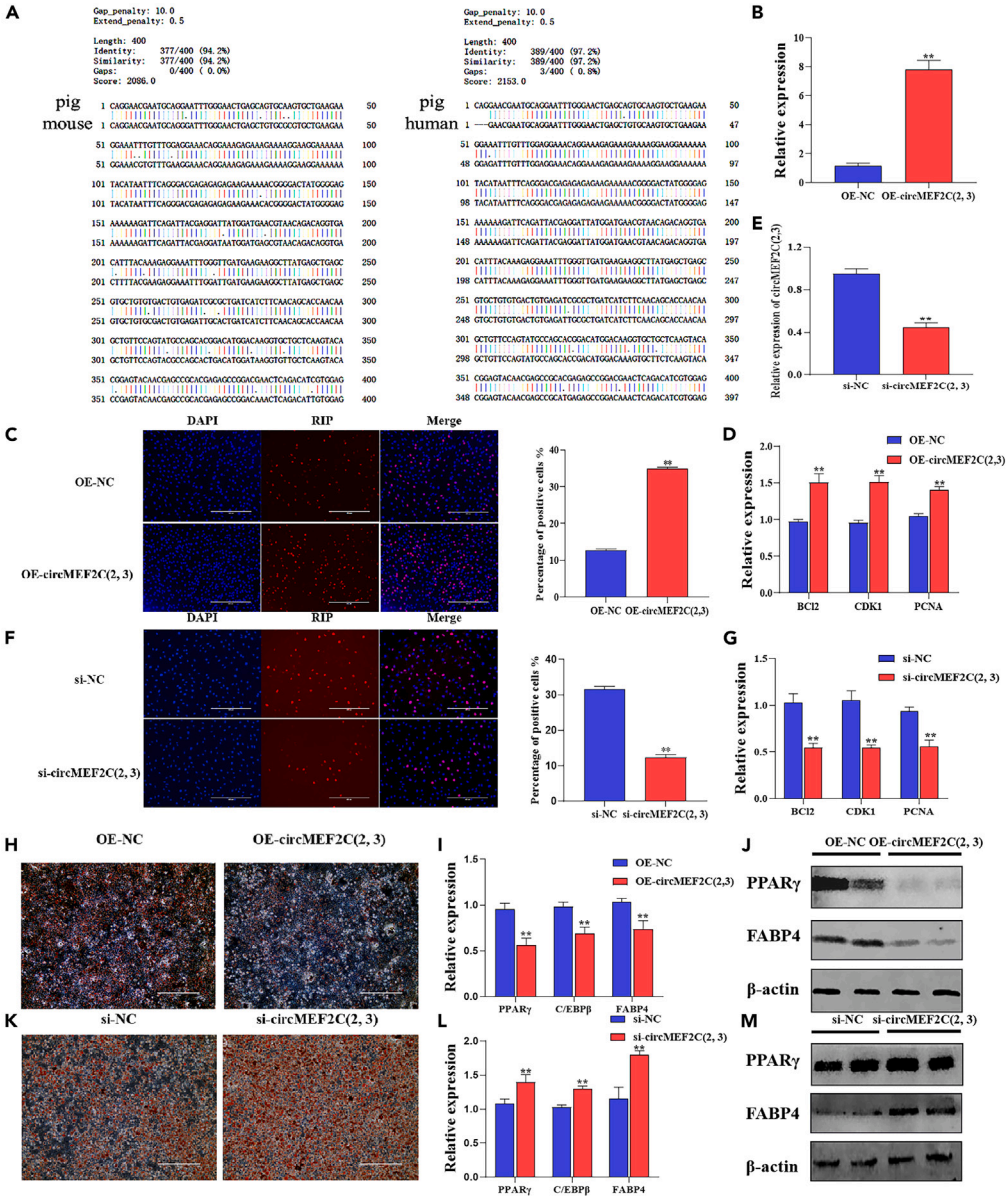

Figure 3. CircMEF2C(2, 3) regulates proliferation and adipogensis in murine C3H10T1/2 cells

(A) Assessment of the homology of porcine circMEF2C(2, 3) with murine and human circMEF2C(2, 3) by DNAMAN software.

(B) Detection of circMEF2C(2, 3) overexpression efficiency in murine C3H10T1/2 cells.

(C) Differences in EdU staining following circMEF2C(2, 3) overexpression.

(D) Alterations in mRNA expression of proliferation-related genes following circMEF2C(2, 3) overexpression.

(E) Evaluation of interference efficiency of si-circMEF2C(2, 3) in murine C3H10T1/2 cells.

(F) Differences in EdU staining following circMEF2C(2, 3) interference.

(G) Alterations in mRNA expression of proliferation-related genes following circMEF2C(2, 3) interference.

(H) Representative results of oil red O staining following circMEF2C(2, 3) overexpression.

(I) Alterations in mRNA expression of adipogenic factors following circMEF2C(2, 3) overexpression.

(J) Alterations in protein expression of adipogenic factors following circMEF2C(2, 3) overexpression.

(K) Representative results of oil red O staining following circMEF2C(2, 3) interference.

(L) Alterations in mRNA expression of adipogenic factors following circMEF2C(2, 3) interference.

(M) Alterations in protein expression of adipogenic factors following circMEF2C(2, 3) interference.

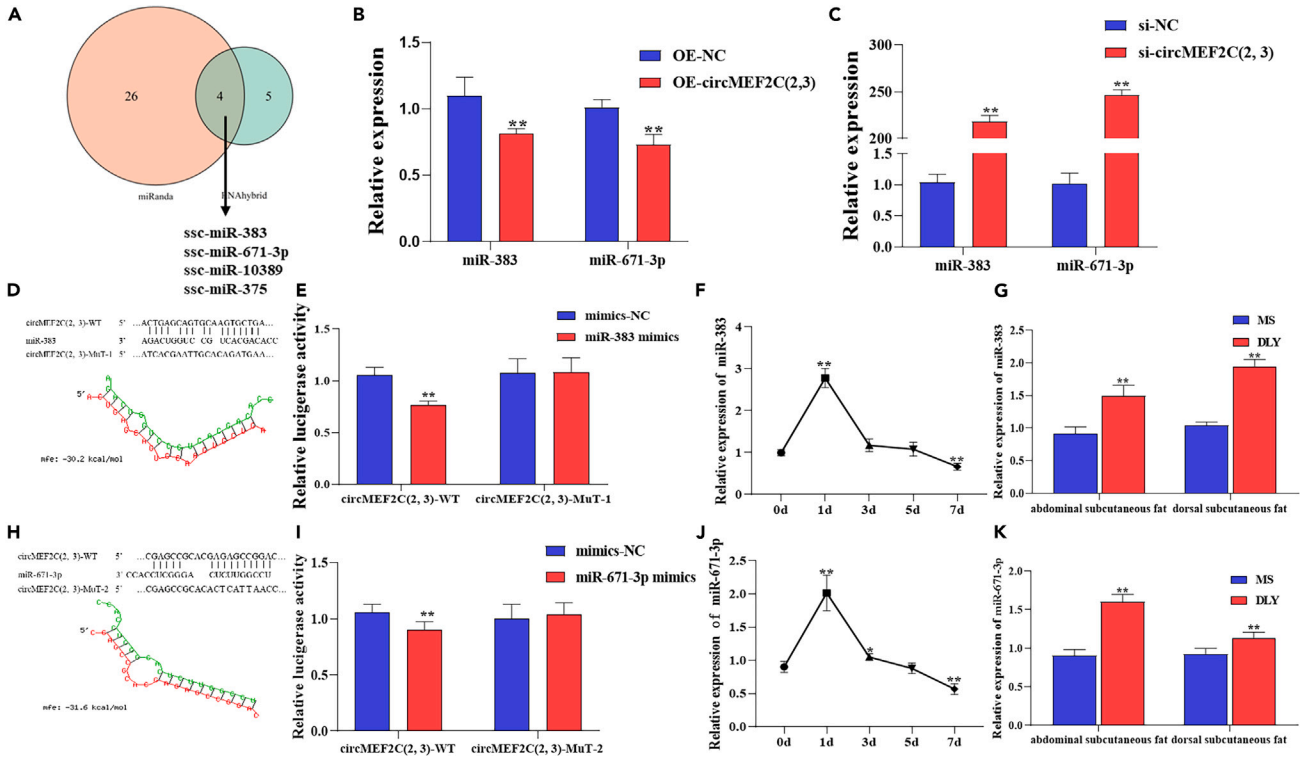

Figure 4. CircMEF2C(2, 3) acts as a miR-383 and miR-671-3p sponge

(A) MiRANda and RNAhybrid databases predict the miRNAs that circMEF2C(2, 3) may bind.

(B and C) Alterations in miR-383 and miR-671-3p expression following circMEF2C(2, 3) overexpression or interference.

(D and H) Prediction of binding sites between circMEF2C(2, 3) and miR-383/miR-671-3p using RNAhybrid software, along with wild-type and mutant-type vector sequences of circMEF2C(2, 3).

(E and I) Dual-luciferase reporter gene assay results.

(F and J) Expression patterns of miR-383 and miR-671-3p during adipogenesis.

(G and K) Expression of miR-383 and miR-671-3p in adipose tissue of MS pigs and DLY pigs.

MEF2C enhances proliferation and restrain adipogenic differentiation

Finally, we examined *MEF2C*'s expression pattern and function. Tissue profiling revealed that *MEF2C* exhibited the highest expression level among the three muscle types (Figure 8A). Furthermore, it was upregulated during late-stage adipogenic differentiation (Figure 8B) and *MEF2C* was detected in different breeds of pigs and it was found that it is expressed more in the muscle of lean pigs (DLY) (Figures 8C and 8D), resembling circMEF2C(2, 3) expression (Figures 1F–1I). To assess *MEF2C*'s impact on porcine intramuscular preadipocytes adipogenic differentiation, we developed siRNA targeting *MEF2C* and assessed its efficacy in interference (Figure 8E). RT-qPCR demonstrates that interference with *MEF2C* promotes the expression of genes related to cell proliferation and suppresses the expression of genes related to adipogenesis (Figures 8F and 8H). Rescue experiments also indicate that the addition of si-*MEF2C* can restore the impact of miR-383 inhibitor or miR-671-3p on cell proliferation and adipogenic differentiation (Figures 8G and 8I). Because MEF2C can be used as a transcription factor and regulate downstream gene transcription, we used the Genomatix base to search that *MEF2C* might bind to the promoters of adipogenic marker genes. RT-qPCR found that interfering with *MEF2C* may promote the expression of *Rb1*, *Hivep2*, *ZFP521* et al. (Figure 8J). These findings jointly suggest that *MEF2C* acts as an accelerator of proliferation and an inhibitor of adipogenic differentiation.

DISCUSSION

Due to the widespread prevalence of obesity globally and the increasing health issues associated with it, concerns about abnormal or excessive accumulation of fat have been raised. Understanding the formation of adipose tissue is of significant scientific importance for human health and the field of medicine. The advent of high-throughput sequencing has generated a wealth of data indicating that ncRNAs play pivotal roles in regulating genes, particularly in various metabolic disorders, including lipid metabolism.[22,23] It has been reported that many circRNAs exhibit high evolutionary conservation among closely related species, and even across distant species.[24] Pigs, as an excellent biomedical model for studying the fundamental mechanisms of adipogenesis, obesity, and obesity-related diseases, are suitable for investigating the biological functions mediated by circRNAs and the regulatory mechanisms of adipogenesis. In this study, we uncovered a

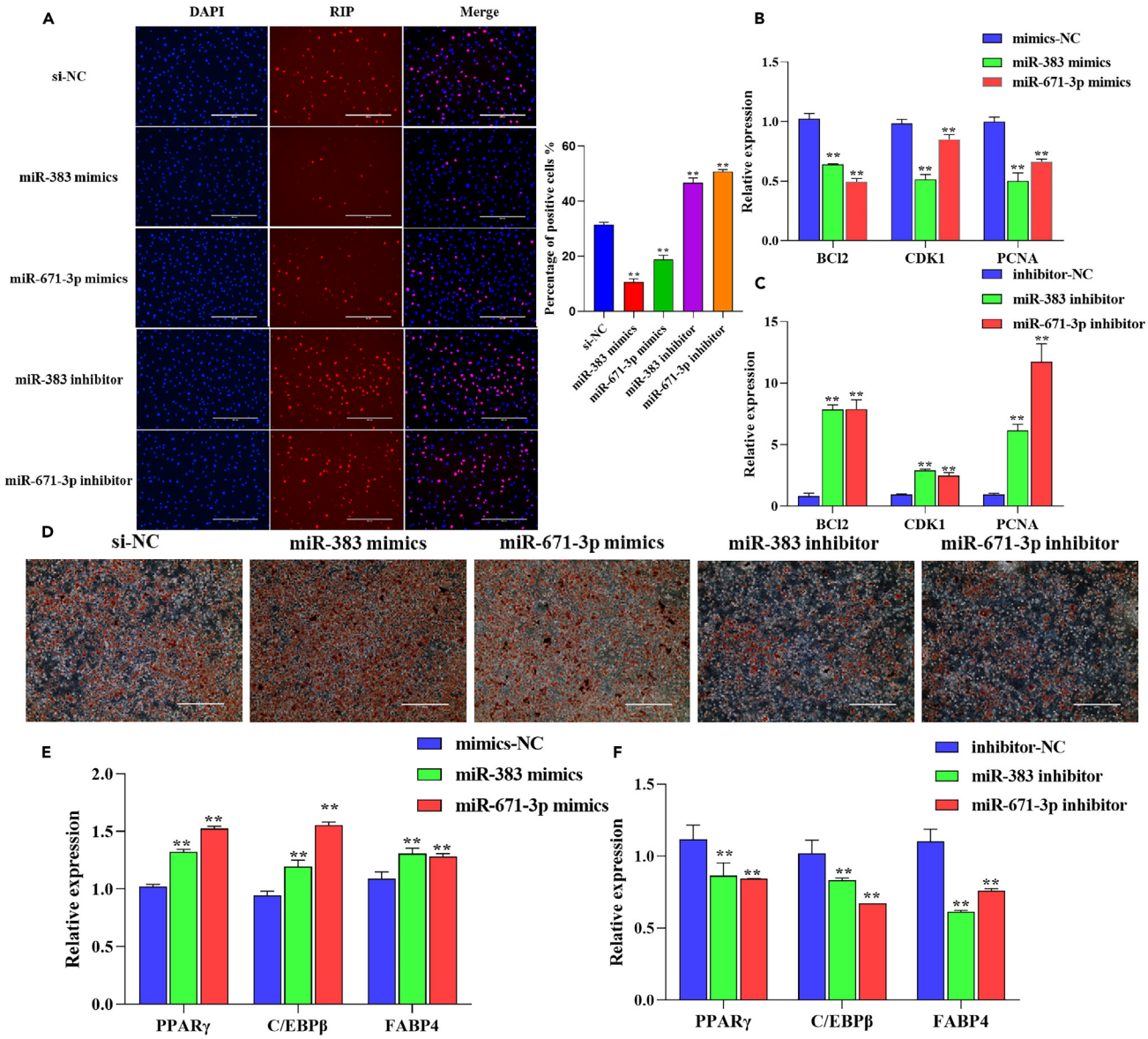

Figure 5. miR-383 and miR-671-3p suppress proliferation and enhance adipogenic differentiation

(A) Differences in EdU staining following miR-383 or miR-671-3p overexpression or interference.

(B) Alterations in mRNA expression of proliferation-related genes following miR-383 or miR-671-3p overexpression.

(C) Alterations in mRNA expression of proliferation-related genes following miR-383 or miR-671-3p interference.

(D) Representative results of oil red O staining following miR-383 or miR-671-3p overexpression or interference.

(E) Alterations in mRNA expression of adipogenic factors following miR-383 or miR-671-3p overexpression.

(F) Alterations in mRNA expression of adipogenic factors following miR-383 or miR-671-3p interference.

regulatory axis involving circMEF2C(2, 3)/miR-383 and miR-671-3p/*MEF2C*, which governs the proliferation and adipogenic differentiation of adipocytes.

The development of adipose tissue is under the control of a cascade of transcription factors, including *PPARγ*,[25,26] and *C/EBPα*.[27] Furthermore, HMG20A, a member of the high-mobility group protein family, plays a crucial role in cell development, differentiation, and proliferation.[28] It is worth noting that HMG20A and LSD1 are core subunits of the CoREST complex, which features prominently in adipose development and metabolic processes. Preliminary findings from our research indicate that *MEF2C* is a target gene downstream of HMG20A, and its expression is subject to regulation by HMG20A and LSD1. This regulatory interplay may hold significant implications in the context of adipogenic differentiation.[20] Our study identified a homologous circRNA of *MEF2C* in porcine intramuscular preadipocytes through a series of experimental procedures. This circRNA originates from exons 2 and 3 of the *MEF2C* gene, and in line with established nomenclature

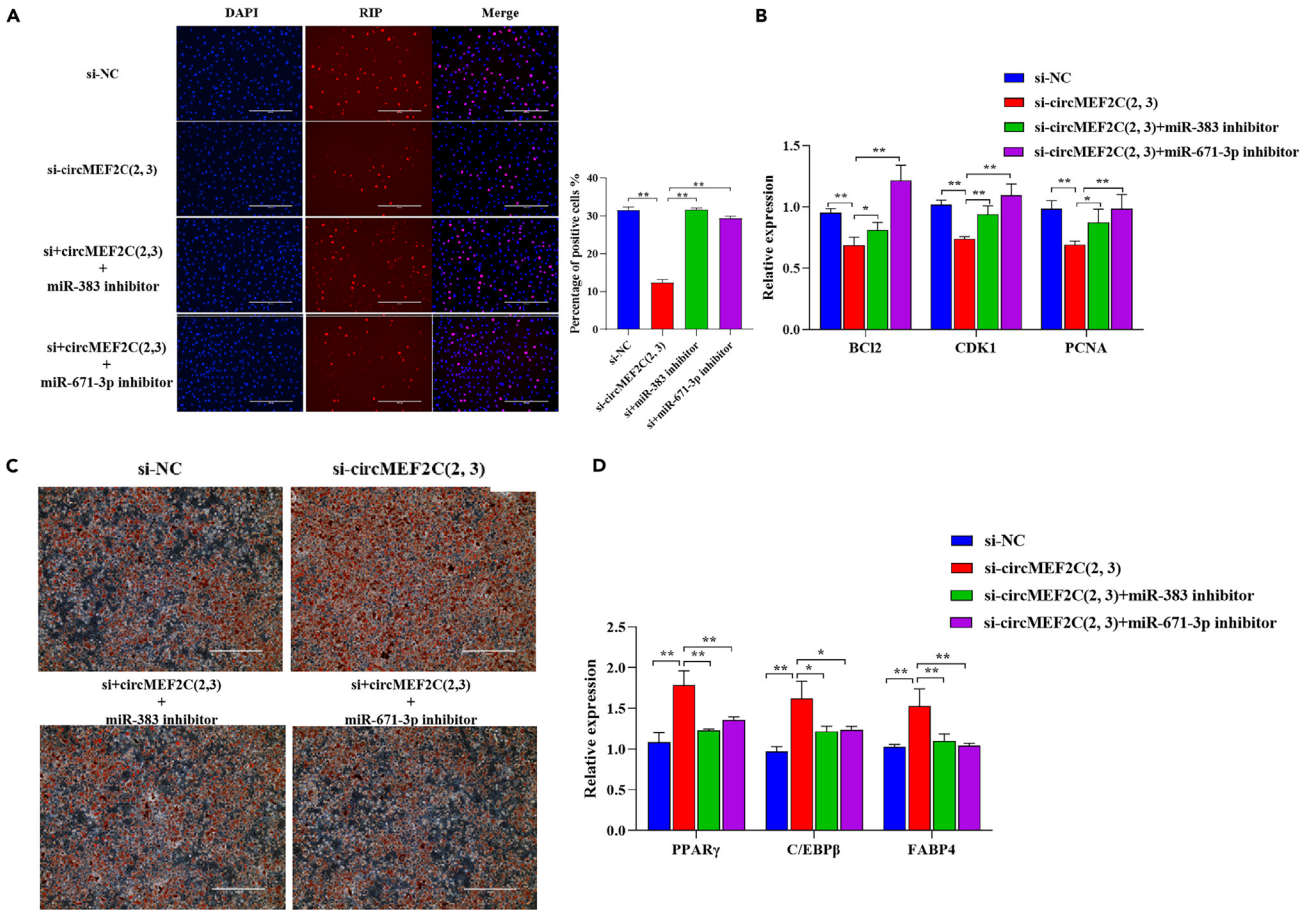

Figure 6. CircMEF2C(2, 3) affects cell proliferation and adipogenesis through miR-383 and miR-671-3p

(A) Differences in EdU staining following cotransfection.

(B) Alterations in mRNA expression of proliferation-related genes following cotransfection.

(C) Representative results of oil red O staining following cotransfection.

(D) Alterations in mRNA expression of adipogenic factors following cotransfection.

principles for circRNAs, we designated it as circMEF2C(2, 3).[29] This finding adds to the understanding of circRNA expression in porcine intramuscular preadipocytes and contributes to the growing body of knowledge regarding circRNA biology.

CircRNAs represent a unique class of ncRNA molecule, known for their remarkable stability, abundant expression, robust conservation, and ubiquitous presence in cells. Extensive research has illuminated the roles circRNAs play in the orchestration of physiological processes, including the regulation of adipose development and muscle formation. For instance, research has elucidated the function of CircH19, which binds to the PTBP1 protein in human adipose-derived stem cells, thereby governing the nuclear-cytoplasmic translocation of the SREBP1 protein and inhibiting adipose generation.[12] In a separate study, it was revealed that CircSETBP1 expedites the differentiation of intramuscular preadipocytes and 3T3-L1 cells by modulating the miR-149-5p/CRTCs axis, consequently curtailing cell proliferation.[30] Through gain or loss-of-function experiments, we have confirmed that circMEF2C(2, 3) exerts a dual regulatory role in porcine intramuscular preadipocytes. Specifically, we observed that circMEF2C(2, 3) enhances cell proliferation while concurrently inhibiting the differentiation of these cells into mature adipocytes. These findings underscore the intricate regulatory mechanisms involving circMEF2C(2, 3) in the context of adipogenesis, shedding light on its potential as a key modulator of cellular processes in intramuscular preadipocytes.

Given the high conservation of circRNAs across species, they are likely to perform analogous biological functions in various organisms. Studies have demonstrated that CircHIPK3, in mouse cells, mitigates cell apoptosis and counteracts mitochondrial dysfunction by serving as a miR-148b-3p sponge.[31] In human cells, on the other hand, CircHIPK3 promotes cell proliferation and migration while slowing down cell apoptosis, all achieved by sequestering miR-382-5p,[32] miR-30a-3p,[33] and miR-124.[34] Consistent with previous research findings, our results corroborate that circMEF2C(2, 3) exhibits a high degree of conservation in pigs and mice, and its identical biological function.

The general consensus in research suggests that when cells are stimulated with adipogenic induction medium, they undergo approximately two rounds of cell division in the first 2–3 days of adipogenic induction, known as the mitotic clonal expansion phase, followed by growth arrest and terminal differentiation.[35,36] However, the question of whether mitotic clonal expansion is a prerequisite for adipogenic

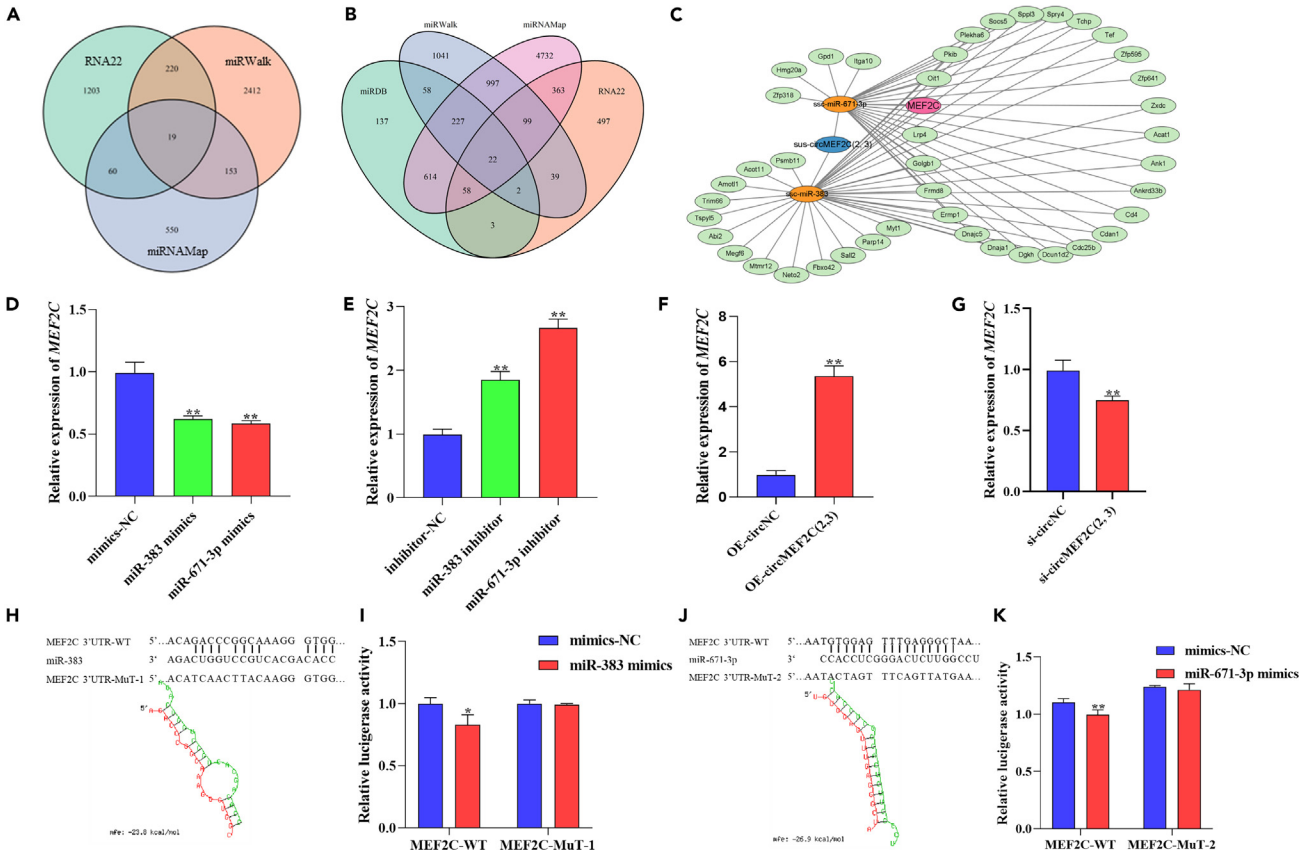

Figure 7. MiR-383 and miR-671-3p bind to the 3′-UTR of *MEF2C*

(A and B) The downstream target genes of miR-383 and miR-671-3p were predicted by RNA22, miRWalk, miRNAMap, and miRDB databases. Venn diagram depicting common target genes of ssc-miR-383 and ssc-miR-671-3p.

(C) Network map illustrating the circMEF2C(2, 3)-miRNA-mRNA interactions.

(D–G) Alterations in *MEF2C* expression after miR-383, miR-671-3p, and circMEF2C(2, 3) overexpression or interference.

(H and J) Predicted binding sites of *MEF2C* with miR-383 and miR-671-3p using RNAhybrid software, and the wild-type and mutant-type vector sequences of *MEF2C*.

(I and K) Dual-luciferase reporter gene assay results.

differentiation has been a topic of debate. There is evidence in the literature that argues against the notion that mitotic clonal expansion is a prerequisite for adipogenesis.[37,38] On the contrary, research indicates a molecular coupling between proliferation arrest and adipogenic differentiation. PPARγ and C/EBPα have been shown to promote cell-cycle arrest by upregulating CDK inhibitors p18 and p21 and inhibiting E2F-dependent transcription.[39,40] Additionally, it has been shown that preadipocytes must cease growth in a unique state of the G1 phase of the cell cycle before expressing the adipogenic differentiation phenotype.[41] Since circMEF2C(2, 3) has a proliferation promoting role in cells, we speculated that it may prevent cells from being unable to end the mitotic clonal expansion stage without growth arrest and terminal differentiation, finally achieving the effect of inhibiting adipogenic differentiation.

In the cytoplasm, circRNAs often serve as "molecular sponges", competitively binding with miRNAs to modulate gene expression. For example, recent research has demonstrated that exosomal hsa_circ_0006859 enhances the adipogenic and osteogenic differentiation of human bone marrow mesenchymal stem cells by sequestering miR-431-5p.[42] In bovine primary adipocytes, circPPARγ promotes adipogenesis while simultaneously inhibiting cell proliferation and apoptosis.[43] Furthermore, previous studies conducted have indicated that circHOMER1 may inhibit adipogenic differentiation in porcine preadipocytes and C3H10T1/2 cells, thereby suppressing adipogenesis in mice through its interaction with SIRT1 via miR-23b.[44,45] This current study provides further confirmation that circMEF2C(2, 3) actively participates in the regulation of adipocyte proliferation and adipogenesis by functioning as a miR-383 and miR-671-3p sponge.

Several studies have highlighted the involvement of circRNAs in the regulation of parental gene expression. Notably, circEIF3J and circPAIP2 engage with U1 snRNP to facilitate the transcription of their respective parental genes.[46] On the other hand, circPABPN1 competes with the mRNA of the parental gene for binding to the HuR protein, thereby inhibiting the translation of PABPN1.[47] In our study, it was established that *MEF2C* is a common target of miR-383 and miR-671-3p, and the circMEF2C(2, 3) modulates the expression of its parental gene, *MEF2C*, through the ceRNA network. Because *MEF2C* can be used as a transcription factor and regulate downstream gene transcription,[48,49]

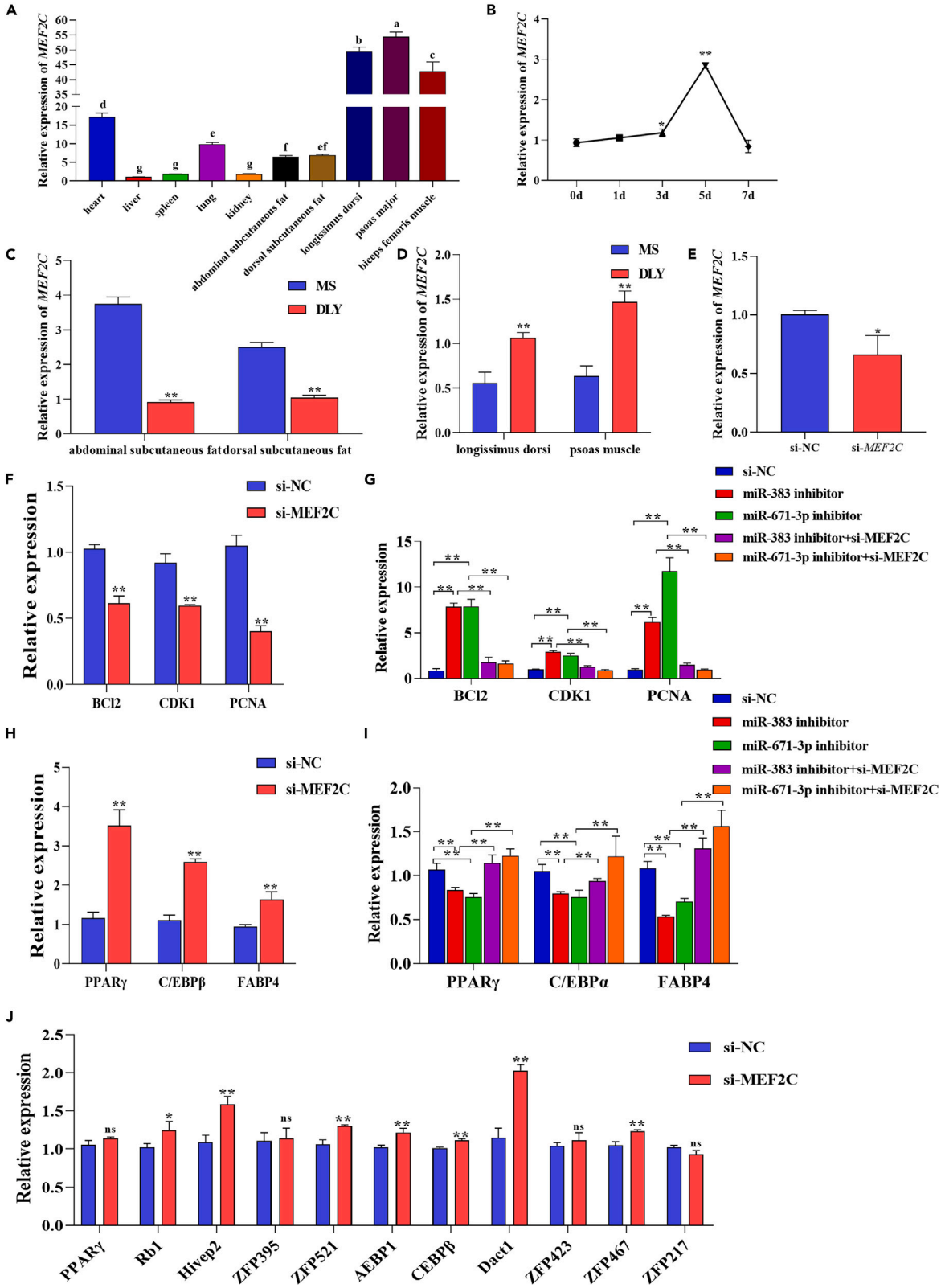
A
Relative expression of MEF2C
heart
liver
spleen
lung
kidney
abdominal subcutaneous fat
dorsal subcutaneous fat
longissimus dorsi
psoas major
biceps femoris muscle
B
Relative expression of MEF2C
0d
1d
3d
5d
7d
C
Relative expression of MEF2C
MS
DLY
abdominal subcutaneous fat
dorsal subcutaneous fat
D
Relative expression of MEF2C
MS
DLY
longissimus dorsi
psoas muscle
E
Relative expression of MEF2C
si-NC
si-MEF2C
F
Relative expression
si-NC
si-MEF2C
BCl2
CDK1
PCNA
G
Relative expression
si-NC
miR-383 inhibitor
miR-671-3p inhibitor
miR-383 inhibitor+si-MEF2C
miR-671-3p inhibitor+si-MEF2C
BCl2
CDK1
PCNA
H
Relative expression
si-NC
si-MEF2C
PPARγ
C/EBPβ
FABP4
I
Relative expression
si-NC
miR-383 inhibitor
miR-671-3p inhibitor
miR-383 inhibitor+si-MEF2C
miR-671-3p inhibitor+si-MEF2C
PPARγ
C/EBPα
FABP4
J
Relative expression
si-NC
si-MEF2C
PPARγ
Rb1
Hivep2
ZFP395
ZFP521
AEBP1
CEBPβ
Dact1
ZFP423
ZFP467
ZFP217

Figure 8. *MEF2C* enhances proliferation and restrain adipogenic differentiation

(A) Tissue expression profile of *MEF2C*.

(B) Expression patterns of *MEF2C* during adipogenesis.

(C) Expression of *MEF2C* in adipose tissue of MS pigs and DLY pigs.

(D) Expression of *MEF2C* in muscle tissue of MS pigs and DLY pigs.

(E) Detection of interference efficiency of si-MEF2C.

(F and G) Alterations in mRNA expression of proliferation factors following *MEF2C* interference and cotransfection.

(H and I) Detection of changes in the mRNA expression of adipogenic factors following *MEF2C* interference and cotransfection after 8 days of adipogenic differentiation.

(J) Expression of adipogenic-related genes after interference with *MEF2C*.

we used the Genomatix base to search that *MEF2C* might bind to the promoters of adipogenic marker genes, affecting their transcription. Then we knocked down the *MEF2C*, RT-qPCR found that interfering with *MEF2C* may promote the expression of *Rb1*, *Hivep2*, *ZFP521* et al. These results suggest that *MEF2C* may act as a transcription factor regulating the transcription of key factors in adipogenesis, but the specific regulatory mechanism still needs further exploration.

In summary, this study has uncovered a key circRNA, circMEF2C(2, 3), derived from the *MEF2C* gene in pigs. CircMEF2C(2,3) can enhance cell proliferation and inhibit the adipogenic differentiation of porcine intramuscular preadipocytes and murine C3H10T1/2 cells. Mechanistic investigations revealed that circMEF2C(2, 3) functions as a ceRNA by binding to miR-383 and miR-671-3p, thereby impacting the expression of the target gene *MEF2C*. These discoveries establish a theoretical foundation for understanding the role and mechanism of circMEF2C(2, 3) in regulating adipogenic differentiation in pigs, with potential implications for improving pork quality and managing related diseases.

Limitations of the study

While our research delved into the experimental verification of circMEF2C(2, 3) functioning as a ceRNA through miR-383 and miR-671-3p, it should be acknowledged that circRNAs can exhibit diverse functions, and there might be additional regulatory mechanisms yet to be explored. Future research should aim to uncover alternative mechanisms through which circMEF2C(2, 3) impacts cell proliferation and adipocyte differentiation, including potential protein interactions or peptide encoding.

STAR★METHODS

Detailed methods are provided in the online version of this paper and include the following:

- KEY RESOURCES TABLE
- RESOURCE AVAILABILITY
  - Lead contact
  - Materials availability
  - Data and code availability
- EXPERIMENTAL MODEL AND STUDY PARTICIPANT DETAILS
  - Sample collection
  - Extraction and culture of porcine intramuscular preadipocytes
- METHOD DETAILS
  - Bioinformatics analysis
  - Total RNA extraction and cDNA synthesis
  - RNase R treatment
  - Nucleoplasmic positioning
  - PCR and RT-qPCR detection
  - Plasmid and siRNA transfection
  - EdU fluorescence staining
  - Oil red O staining
  - Protein extraction and western blot analysis
  - Dual-luciferase Reporter Assay
- QUANTIFICATION AND STATISTICAL ANALYSIS

ACKNOWLEDGMENTS

This work was supported by National Natural Science Foundation of China (32272846), Graduate Student Innovation Project of Shanxi Province (2022Y342), Key Research and Development Project of Shanxi Province (202102140601005), Key Laboratory Open Fund of Farm Animal Genetic Resources Exploration and Breeding of Shanxi Province, Pig Seed Industry Innovation Varieties Joint Research of Shanxi Province (YZGG-06).

AUTHOR CONTRIBUTIONS

The article was drafted by X.R. and R.L. The concept for this study's design was created by X.R., R.L., X.G., and Y.Y. The experiment was finished and the data were examined by T.G., H.L., and X.Z. The data were processed and ideas were supplemented by G.C., M.L., and B.L. The data as well as the article were corrected by X.G. and Y.Y. The final article was read and approved by all authors.

DECLARATION OF INTERESTS

The authors declare no competing interests.

Received: November 14, 2023
Revised: February 6, 2024
Accepted: April 6, 2024
Published: April 10, 2024

REFERENCES

1. Hotamisligil, G.S. (2006). Inflammation and metabolic disorders. Nature *444*, 860–867.
2. Trayhurn, P. (2005). Adipose tissue in obesity—an inflammatory issue. Endocrinology *146*, 1003–1005.
3. Hocquette, J.F., Gondret, F., Baéza, E., Médale, F., Jurie, C., and Pethick, D.W. (2010). Intramuscular fat content in meat-producing animals: development, genetic and nutritional control, and identification of putative markers. Animal *4*, 303–319.
4. Poleti, M.D., Regitano, L.C.A., Souza, G.H.M.F., Cesar, A.S.M., Simas, R.C., Silva-Vignato, B., Oliveira, G.B., Andrade, S.C.S., Cameron, L.C., and Coutinho, L.L. (2018). Longissimus dorsi muscle label-free quantitative proteomic reveals biological mechanisms associated with intramuscular fat deposition. J. Proteonomics *179*, 30–41.
5. Gu, H., Zhou, Y., Yang, J., Li, J., Peng, Y., Zhang, X., Miao, Y., Jiang, W., Bu, G., Hou, L., et al. (2021). Targeted overexpression of PPARγ in skeletal muscle by random insertion and CRISPR/Cas9 transgenic pig cloning enhances oxidative fiber formation and intramuscular fat deposition. FASEB J. *35*, e21308.
6. Wood, J.D., Enser, M., Fisher, A.V., Nute, G.R., Sheard, P.R., Richardson, R.I., Hughes, S.I., and Whittington, F.M. (2008). Fat deposition, fatty acid composition and meat quality: A review. Meat Sci. *78*, 343–358.
7. Ambele, M.A., Dhanraj, P., Giles, R., and Pepper, M.S. (2020). Adipogenesis: a complex interplay of multiple molecular determinants and pathways. Int. J. Mol. Sci. *21*, 4283.
8. Ong, C.-T., and Corces, V.G. (2011). Enhancer function: new insights into the regulation of tissue-specific gene expression. Nat. Rev. Genet. *12*, 283–293.
9. Chen, L.-L., and Yang, L. (2015). Regulation of circRNA biogenesis. RNA Biol. *12*, 381–388.
10. Zeng, K., Chen, X., Xu, M., Liu, X., Hu, X., Xu, T., Sun, H., Pan, Y., He, B., and Wang, S. (2018). CircHIPK3 promotes colorectal cancer growth and metastasis by sponging miR-7. Cell Death Dis. *9*, 417.
11. Shen, S., Wu, Y., Chen, J., Xie, Z., Huang, K., Wang, G., Yang, Y., Ni, W., Chen, Z., Shi, P., et al. (2019). CircSERPINE2 protects against osteoarthritis by targeting miR-1271 and ETS-related gene. Ann. Rheum. Dis. *78*, 826–836.
12. Zhu, Y., Gui, W., Lin, X., and Li, H. (2020). Knock-down of circular RNA H19 induces human adipose-derived stem cells adipogenic differentiation via a mechanism involving the polypyrimidine tract-binding protein 1. Exp. Cell Res. *387*, 111753.
13. Chen, R.-X., Chen, X., Xia, L.-P., Zhang, J.-X., Pan, Z.-Z., Ma, X.-D., Han, K., Chen, J.-W., Judde, J.-G., Deas, O., et al. (2019). N 6-methyladenosine modification of circNSUN2 facilitates cytoplasmic export and stabilizes HMGA2 to promote colorectal liver metastasis. Nat. Commun. *10*, 4695.
14. Holdt, L.M., Stahringer, A., Sass, K., Pichler, G., Kulak, N.A., Wilfert, W., Kohlmaier, A., Herbst, A., Northoff, B.H., Nicolaou, A., et al. (2016). Circular non-coding RNA ANRIL modulates ribosomal RNA maturation and atherosclerosis in humans. Nat. Commun. *7*, 12429.
15. Yang, Y., Gao, X., Zhang, M., Yan, S., Sun, C., Xiao, F., Huang, N., Yang, X., Zhao, K., Zhou, H., et al. (2018). Novel role of FBXW7 circular RNA in repressing glioma tumorigenesis. J. Natl. Cancer Inst. *110*, 304–315.
16. Li, B., He, Y., Wu, W., Tan, X., Wang, Z., Irwin, D.M., Wang, Z., and Zhang, S. (2022). Circular RNA profiling identifies novel circPPARA that promotes intramuscular fat deposition in pigs. J. Agric. Food Chem. *70*, 4123–4137.
17. Wang, W., Org, T., Montel-Hagen, A., Pioli, P.D., Duan, D., Israely, E., Malkin, D., Su, T., Flach, J., Kurdistani, S.K., et al. (2016). MEF2C protects bone marrow B-lymphoid progenitors during stress haematopoiesis. Nat. Commun. *7*, 12376.
18. Fujii, T., Murata, K., Mun, S.-H., Bae, S., Lee, Y.J., Pannellini, T., Kang, K., Oliver, D., Park-Min, K.-H., and Ivashkiv, L.B. (2021). MEF2C regulates osteoclastogenesis and pathologic bone resorption via c-FOS. Bone Res. *9*, 4.
19. Sekiyama, Y., Suzuki, H., and Tsukahara, T. (2012). Functional gene expression analysis of tissue-specific isoforms of Mef2c. Cell. Mol. Neurobiol. *32*, 129–139.
20. Li, R., Meng, S., Ji, M., Rong, X., You, Z., Cai, C., Guo, X., Lu, C., Liang, G., Cao, G., et al. (2022). HMG20A inhibit adipogenesis by transcriptional and epigenetic regulation of MEF2C expression. Int. J. Mol. Sci. *23*, 10559.
21. Li, M., Zhang, N., Li, J., Ji, M., Zhao, T., An, J., Cai, C., Yang, Y., Gao, P., Cao, G., et al. (2023). CircRNA Profiling of Skeletal Muscle in Two Pig Breeds Reveals CircIGF1R Regulates Myoblast Differentiation via miR-16. Int. J. Mol. Sci. *24*, 3779.
22. Agbu, P., and Carthew, R.W. (2021). MicroRNA-mediated regulation of glucose and lipid metabolism. Nat. Rev. Mol. Cell Biol. *22*, 425–438.
23. Li, C., Ni, Y.-Q., Xu, H., Xiang, Q.-Y., Zhao, Y., Zhan, J.-K., He, J.-Y., Li, S., and Liu, Y.-S. (2021). Roles and mechanisms of exosomal non-coding RNAs in human health and diseases. Signal Transduct. Targeted Ther. *6*, 383.
24. Wu, W., Ji, P., and Zhao, F. (2020). CircAtlas: an integrated resource of one million highly accurate circular RNAs from 1070 vertebrate transcriptomes. Genome Biol. *21*, 101–114.
25. Tamori, Y., Masugi, J., Nishino, N., and Kasuga, M. (2002). Role of peroxisome proliferator-activated receptor-γ in maintenance of the characteristics of mature 3T3-L1 adipocytes. Diabetes *51*, 2045–2055.
26. Rosen, E.D., and MacDougald, O.A. (2006). Adipocyte differentiation from the inside out. Nat. Rev. Mol. Cell Biol. *7*, 885–896.
27. Lefterova, M.I., Zhang, Y., Steger, D.J., Schupp, M., Schug, J., Cristancho, A., Feng, D., Zhuo, D., Stoeckert, C.J., Liu, X.S., and Lazar, M.A. (2008). PPARγ and C/EBP factors orchestrate adipocyte biology via adjacent binding on a genome-wide scale. Genes Dev. *22*, 2941–2952.
28. Gómez-Marín, E., Posavec-Marjanović, M., Zarzuela, L., Basurto-Cayuela, L., Guerrero-Martínez, J.A., Arribas, G., Yerbes, R., Ceballos-Chávez, M., Rodríguez-Paredes, M., Tomé, M., et al. (2022). The high mobility group protein HMG20A cooperates with the histone reader PHF14 to modulate TGFβ and Hippo pathways. Nucleic Acids Res. *50*, 9838–9857.
29. Chen, L.-L., Bindereif, A., Bozzoni, I., Chang, H.Y., Matera, A.G., Gorospe, M., Hansen, T.B., Kjems, J., Ma, X.-K., Pek, J.W., et al. (2023). A guide to naming eukaryotic circular RNAs. Nat. Cell Biol. *25*, 1–5.
30. Liu, Y., Dou, Y., Qi, K., Li, C., Song, C., Li, X., Li, X., Qiao, R., Wang, K., and Han, X. (2022). CircSETBP1 Acts as a MiR-149-5p sponge to promote intramuscular Fat deposition by regulating CRTCs. J. Agric. Food Chem. *70*, 12841–12851.
31. Chen, G., Shan, X., Li, L., Dong, L., Huang, G., and Tao, H. (2022). circHIPK3 regulates apoptosis and mitochondrial dysfunction induced by ischemic stroke in mice by sponging miR-148b-3p via CDK5R1/SIRT1. Exp. Neurol. *355*, 114115.
32. Yin, X., Zheng, W., He, L., Mu, S., Shen, Y., and Wang, J. (2022). CircHIPK3 alleviates inflammatory response and neuronal apoptosis via regulating miR-382-5p/DUSP1 axis in spinal cord injury. Transpl. Immunol. *73*, 101612.

33. Shang, J., Li, H., Wu, B., Jiang, N., Wang, B., Wang, D., Zhong, J., Chen, Y., Xu, X., and Lu, H. (2022). CircHIPK3 prevents chondrocyte apoptosis and cartilage degradation by sponging miR-30a-3p and promoting PON2. Cell Prolif. *55*, e13285.
34. Yao, D., Lin, S., Chen, S., and Wang, Z. (2022). circHIPK3 regulates cell proliferation and migration by sponging microRNA-124 and regulating serine/threonine kinase 3 expression in esophageal squamous cell carcinoma. Bioengineered *13*, 9767–9780.
35. Qiu, Z., Wei, Y., Chen, N., Jiang, M., Wu, J., and Liao, K. (2001). DNA synthesis and mitotic clonal expansion is not a required step for 3T3-L1 preadipocyte differentiation into adipocytes. J. Biol. Chem. *276*, 11988–11995.
36. Tang, Q.-Q., Otto, T.C., and Lane, M.D. (2003). Mitotic clonal expansion: a synchronous process required for adipogenesis. Proc. Natl. Acad. Sci. USA *100*, 44–49.
37. Prusty, D., Park, B.-H., Davis, K.E., and Farmer, S.R. (2002). Activation of MEK/ERK signaling promotes adipogenesis by enhancing peroxisome proliferator-activated receptor γ (PPARγ) and C/EBPα gene expression during the differentiation of 3T3-L1 preadipocytes. J. Biol. Chem. *277*, 46226–46232.
38. McBeath, R., Pirone, D.M., Nelson, C.M., Bhadriraju, K., and Chen, C.S. (2004). Cell shape, cytoskeletal tension, and RhoA regulate stem cell lineage commitment. Dev. Cell *6*, 483–495.
39. Morrison, R.F., and Farmer, S.R. (1999). Role of PPARγ in regulating a cascade expression of cyclin-dependent kinase inhibitors, p18 (INK4c) and p21 (Waf1/Cip1), during adipogenesis. J. Biol. Chem. *274*, 17088–17097.
40. Slomiany, B.A., D'Arigo, K.L., Kelly, M.M., and Kurtz, D.T. (2000). C/EBPα inhibits cell growth via direct repression of E2F-DP-mediated transcription. Mol. Cell Biol. *20*, 5986–5997.
41. Scott, R.E., Hoerl, B.J., Wille, J.J., Jr., Florine, D.L., Krawisz, B.R., and Yun, K. (1982). Coupling of proadipocyte growth arrest and differentiation. II. A cell cycle model for the physiological control of cell proliferation. J. Cell Biol. *94*, 400–405.
42. Zhi, F., Ding, Y., Wang, R., Yang, Y., Luo, K., and Hua, F. (2021). Exosomal hsa_circ_0006859 is a potential biomarker for postmenopausal osteoporosis and enhances adipogenic versus osteogenic differentiation in human bone marrow mesenchymal stem cells by sponging miR-431-5p. Stem Cell Res. Ther. *12*, 157–215.
43. Wu, J., Zhang, S., Yue, B., Zhang, S., Jiang, E., Chen, H., and Lan, X. (2022). CircRNA profiling reveals CircPPARγ modulates Adipogenic differentiation via sponging miR-92a-3p. J. Agric. Food Chem. *70*, 6698–6708.
44. Li, M., Li, J., Ji, M., An, J., Zhao, T., Yang, Y., Cai, C., Gao, P., Cao, G., Guo, X., and Li, B. (2023). CircHOMER1 inhibits porcine adipogenesis via the miR-23b/SIRT1 axis. Faseb. J. *37*, e22828.
45. Li, M., Zhang, N., Li, J., Zhang, W., Hei, W., Ji, M., Yang, Y., Cao, G., Guo, X., and Li, B. (2022). MiR-23b promotes porcine preadipocyte differentiation via SESN3 and ACSL4. Cells *11*, 2339.
46. Li, Z., Huang, C., Bao, C., Chen, L., Lin, M., Wang, X., Zhong, G., Yu, B., Hu, W., Dai, L., et al. (2015). Exon-intron circular RNAs regulate transcription in the nucleus. Nat. Struct. Mol. Biol. *22*, 256–264.
47. Abdelmohsen, K., Panda, A.C., Munk, R., Grammatikakis, I., Dudekula, D.B., De, S., Kim, J., Noh, J.H., Kim, K.M., Martindale, J.L., and Gorospe, M. (2017). Identification of HuR target circular RNAs uncovers suppression of PABPN1 translation by CircPABPN1. RNA Biol. *14*, 361–369.
48. Han, J., Jiang, Y., Li, Z., Kravchenko, V.V., and Ulevitch, R.J. (1997). Activation of the transcription factor MEF2C by the MAP kinase p38 in inflammation. Nature *386*, 296–299.
49. Udeochu, J.C., Amin, S., Huang, Y., Fan, L., Torres, E.R.S., Carling, G.K., Liu, B., McGurran, H., Coronas-Samano, G., Kauwe, G., et al. (2023). Tau activation of microglial cGAS–IFN reduces MEF2C-mediated cognitive resilience. Nat. Neurosci. *26*, 737–750.

STAR★METHODS

KEY RESOURCES TABLE

REAGENT or RESOURCE	SOURCE	IDENTIFIER
Biological samples		
MaShen (MS) pigs	Animal experimental station of Shanxi Agricultural University	N/A
Duroc × Landrace × Yorkshire (DLY) pigs	Animal experimental station of Shanxi Agricultural University	N/A
Chemicals, peptides, and recombinant proteins		
Actinomycin D	MedChemExpress	Cat#HY-17559
TRIzol Reagent	Thermo Fisher Scientific	1559606
DMEM	Gibco	11965092
Fetal Bovine Serum	Gibco	16140071
Dexamethasone	Aladdin	D137736
3-Isobutyl-1-methylxanthine (IBMX)	Aladdin	I106812
Insulin	Aladdin	I189675
Oil Red O	Solarbio	G1262
Lipofectamine 3000	Thermo Fisher Scientific	L3000150
Collagen Type I	Gibco	17100017
RIPA buffer	Solarbio	R0010
BCA kit	Beyotime	P0010S
PVDF membranes	Millipore	IPVHO0010
β-actin Rabbit mAb	Abclonal	RRID: AB_2863784
PPARγ Rabbit pAb	Abclonal	RRID: AB_2758449
FABP4 Rabbit pAb	Abclonal	RRID: AB_2757045
Critical commercial assays		
PrimeScript™ RT reagent Kit with gDNA Eraser	Takara	RR047A
Taq Master Mix	Vazyme	P112
SmartChip® Real-Time PCR System	Takara	640022
Ribonuclease R (RNase R)	Geneseed	R0301
EdU Cell Proliferation Kit	Sangon Biotech	E607204
Dual-Luciferase Assay kit	Promega	Cat#E1910
Experimental models: Cell lines		
Porcine intramuscular preadipocytes	Isolated from the pig muscle tissue	N/A
Murine C3H10T1/2 cells	Cell Bank of Type Culture Collection of the Chinese Academy of Sciences	N/A
Oligonucleotides		
circMEF2C(2, 3) F: TCATCTTCAACAGCACCAA R: ATTTCCTTCTTCAGCACTTG	This paper	N/A
U6 F: CTCGCTTCGGCAGCACA R:AACGCTTCACGAATTTGCGT	This paper	N/A
18 s F:ATAAACGATGCCGACTGGCGAT R:CAATCTGTCAATCCTGTCCGTGT	This paper	N/A

(*Continued on next page*)

Continued

REAGENT or RESOURCE	SOURCE	IDENTIFIER
GAPDH F: TCGGAGTGAACGGATTTGGC R: TGACAAGCTTCCCGTTCTCC	This paper	N/A
MEF2C F:CCCGATGCAGACGATTCAGT R:GGAGGTGGAACAGCACACAA	This paper	N/A
Mmu-*β-actin* F:CCAGGTCATCACCATCGG R: CCGTGTTGGCGTAGAGGT	This paper	N/A
Mmu-*BCl2* F: CGGTCGCCATGGATCGG R: ATCTGTTCTGGGGCACCATT	This paper	N/A
Mmu-*CDK1* F:AACCACTTTTCCACGGGGATTCA R:GCTAGGCTTCCTGGTTTCCACTTG	This paper	N/A
Mmu-*PCNA* F:TGTAGCCGCGTCGTTGTGATTC R: CGCTTCCAGCACCTTCTTCAGG	This paper	N/A
Mmu-*PPARγ* F: TGGGTGAAACTCTGGGAGATTC R: AGAGGTCCACAGAGCTGATTCC	This paper	N/A
Mmu-*FABP4* F: GATGCCTTTGTGGGAACCTG R: TCCTGTCGTCTGCGGTGATT	This paper	N/A
Mmu-*C/EBPα* F: GCTGAGCGACGAGTACAAGA R: GCTTGAACAAGTTCCGCAGG	This paper	N/A
Sus-*PPARγ* F:AGAGTATGCCAAGAACATCC R:AGGTCGCTGTCATCTAATTC	This paper	N/A
Sus-*FABP4* F:AAGTCAAGAGCACCATAACC R:GATACATTCCACCACCAACT	This paper	N/A
Sus-*C/EBPα* F:AGCCAAGAAGTCGGTAGA R:CGGTCATTGTCACTGGTC	This paper	N/A
Sus-*C/EBPβ* F:AAGAGTAAGACCAAGAAGACC R:GCTCCAGGACCTTATGCT	This paper	N/A
Sus-miR-383 F: CACAGCACTGCCTGGTCAG	This paper	N/A
Sus-miR-671-3p F: CCGGTTCTCAGGGCTCCA	This paper	N/A
Negative Control F: UUCUCCGAACGUGUCACGUTT R: ACGUGACACGUUCGGAGAATT	This paper	N/A
si-circMEF2C(2, 3) F: GGACGAGAGAGAGAAGAAATT R: UUUCUUCUCUCUCGUCCTT	This paper	N/A
miR-383 mimics F: CCACAGCACUGCCUGGUCAGA R: UGACCAGGCAGUGCUGUGGUU	This paper	N/A
miR-671-3p mimics F: UCCGGUUCUCAGGGCUCCACC R: UGGAGCCCUGAGAACCGGAUU	This paper	N/A
miR-383 inhibit F: UCUGACCAGGCAGUGCUGUGGU	This paper	N/A

(*Continued on next page*)

Continued

REAGENT or RESOURCE	SOURCE	IDENTIFIER
miR-671-3p inhibit F: GGUGGAGCCCUGAGAACCGGAU	This paper	N/A
si-MEF2C-1 F: CCAGCACUGACAUGGAUAATT R: UUAUCCAUGUCAGUGCUGGTT	This paper	N/A
si-MEF2C-2 F: GUGGAGACAUUGAGAAAGATT R: UCUUUCUCAAUGUCUCCACTT	This paper	N/A
si-MEF2C-3 F: CACCUGGUAACCUGAACAATT R: UUGUUCAGGUUACCAGGUGTT	This paper	N/A
Software and algorithms		
SPSS 22.0	IBM	N/A

RESOURCE AVAILABILITY

Lead contact

Further information and requests for resources and reagents should be directed to and will be fulfilled by the lead contact, Xiaohong Guo (g_xiaohong@126.com).

Materials availability

The study did not generate new unique reagents.

Data and code availability

- This paper does not report original code.
- Any additional information required to reanalyze the data reported in this paper is available from the lead contact upon request.

EXPERIMENTAL MODEL AND STUDY PARTICIPANT DETAILS

Sample collection

This study received ethical approval from the Animal Ethics Committee of Shanxi Agricultural University. We obtained tissues from three 30-day-old MaShen (MS, castrated boars) pigs as obese pigs and Duroc × Landrace × Yorkshire (DLY, castrated boars) as lean pigs by humane euthanasia through electric shock and exsanguination. The harvested tissues including the heart, liver, spleen, lungs, kidneys, jejunum, abdominal subcutaneous fat, dorsal subcutaneous fat, longest dorsal and psoas muscle, were promptly flash-frozen in liquid nitrogen and stored at −80°C for preservation.

Extraction and culture of porcine intramuscular preadipocytes

Porcine intramuscular preadipocytes were primarily isolated from muscle adipose tissue. In the process, newborn MS piglets (0 days old, boars) were humanly euthanized through electric shock and exsanguination. Subsequently, the longest dorsal muscle tissue was collected under stringent sterile conditions, and thoroughly washed. The tissue was enzymatically digested using 2 mg/mL collagen type I (Gibco) for 2 h, and the digestion process was terminated by introducing a medium containing 10% fetal bovine serum (FBS, Gibco). After filtration through 70 μm and 40μm mesh filters, the resulting cell suspension was seeded into 60 mm culture dishes and placed in a CO_2 incubator at 37°C with 5% CO_2 and 95% O_2 for further cultivation.

METHOD DETAILS

Bioinformatics analysis

Candidates circRNAs sequences were searched through the NCBI (https://www.ncbi.nlm.nih.gov/) and circAtlas 2.0 (http://circatlas.biols.ac.cn/) websites, followed by sequence analysis and positional information alignment using the Ensembl (http://asia.ensembl.org/index.html) Website.

miRanda and RNAhybrid software were utilized to predict circRNA binding miRNAs, miRWalk, miRNAMap, miRDB and RNA22 software were used to predict miRNAs target genes, and their binding sites were predicted using the RNAhybrid web version (https://bibiserv.cebitec.uni-bielefeld.de/rnahybrid/submission.html/).

Total RNA extraction and cDNA synthesis

Total RNA was extracted from tissues or cells in accordance with the guidelines provided by the Trizol reagent kit (Thermo Fisher Scientific). After determining the RNA concentration and purity, the extracted RNA was preserved at −80°C. Subsequently, cDNA was synthesized from mRNA employing the PrimeScrip RT kit (Takara).

RNase R treatment

Total RNA underwent treatment with or without 20 U/μl RNase R (Geneseed) at 37°C for 30 min, after which the reaction was terminated by incubating at 70°C for 10 min to inactivate the enzyme. Subsequently, cDNA was synthesized from this RNase R-treated fraction using the PrimeScript RT Master kit (Takara).

Nucleoplasmic positioning

Total RNA was extracted from the cells using Trizol reagent kit (Thermo Fisher Scientific). To fractionate the nucleus and cytoplasm of cells, Cytoplasmic and Nuclear Extraction Reagents (Thermo Fisher Scientific) were employed. The cytoplasmic fraction was labeled using GAPDH, while the nuclear fraction was labeled using U6.

PCR and RT-qPCR detection

The extracted RNA underwent reverse transcription to generate cDNA with random primers, using the PrimeScript RT Master kit (Takara). PCR, using both cDNA and gDNA, was conducted utilizing the Taq Master Mix (Vazyme). For RT-qPCR, the SmartChip Real-Time PCR System (Takara), was employed. As a reference gene, 18S rRNA or β-actin was utilized, and each sample underwent triplicate testing. The quantification data were calculated using the $2^{-\Delta\Delta Ct}$ method. The primers used in this study were synthesized by Sangon Biotech (Shanghai) Co., Ltd., (Shanghai, China), and their sequences are provided in the key resources table.

Plasmid and siRNA transfection

For overexpressing circMEF2C(2, 3) (OE-circMEF2C(2, 3)), the complete sequence of circMEF2C(2, 3) was amplified and subsequently ligated into the overexpression vector pCD2.1-CIR. To perform interference with circMEF2C(2, 3) (OE-circMEF2C(2, 3)) or *MEF2C* (OE-MEF2C), synthetic siRNA oligonucleotides targeting specific regions within the pig circMEF2C(2, 3) mRNA were designed and synthesized by GenePharma. Additionally, mimics and inhibitors of miR-383 and miR-671-3p were synthesized by GenePharma. For transfection purposes, Lipofectamine 3000 (Thermo Fisher Scientific) was used as the transfection reagent. Detailed sequence information can be found in the key resources table.

EdU fluorescence staining

The EdU (5-ethynyl-2′-deoxyuridine) fluorescence staining method was employed to label proliferating cells. This procedure adhered to the guidelines outlined in the EdU DNA Cell Proliferation Kit (Sangon Biotech, China). Subsequently, fluorescence microscopy was utilized to capture the fluorescence signals and acquire photographic images.

Oil red O staining

Cells underwent two consecutive washes with phosphate-buffered saline (PBS), before being fixed at room temperature for 30 min using 4% paraformaldehyde. They were then immersed in 60% isopropanol for 1 min. After the isopropanol was removed, the cells were treated with a filtered oil red O working solution, which consisted of saturated oil red O dye mixed with distilled water in a 3:2 ratio (Solarbio), for a staining duration of 10 min. After staining, the cells were rinsed with PBS, and images were captured using a microscope.

Protein extraction and western blot analysis

Cells were lysed in RIPA buffer supplemented with protease and phosphatase inhibitor mixture (Solarbio) and vortexed briefly. The supernatant was collected after centrifugation at 15,000 g for 15 min at 4°C. Protein concentrations of the cell lysates were determined using BCA kit (Beyotime).Total proteins were isolated from adipose tissues and cells on day 8 of adipogenic differentiation. Then, the proteins were separated by 10% SDS-PAGE and transferred to PVDF membranes (Millipore). The membranes were incubated overnight at 4°C with primary antibodies specific for β-actin, PPARγ, and FABP4 (1:1000; Abdonal). After incubation with the secondary antibody, the membranes were exposed and photographed.

Dual-luciferase Reporter Assay

The procedures were conducted following the guidelines outlined in the Dual-luciferase Reporter Assay kit (Promega). The ratio of renilla luciferase fluorescence to firefly luciferase fluorescence was calculated to assess the binding between miRNA and circRNA/mRNA.

QUANTIFICATION AND STATISTICAL ANALYSIS

All data are expressed as mean ± standard deviation. Statistical analysis was performed using SPSS 22.0 software (IBM Corp., Armonk, NY, USA). The t-test was employed to evaluate variations between two groups. One-way analysis of variance (ANOVA) was utilized to compare distinctions among three or more groups. Significant differences were denoted by * at the 0.05 significance level and by ** at the 0.01 significance level.